International Journal of Power Electronics and Drive System (IJPEDS)
Vol. 17, No. 4, December 2026, pp. 2570~2580
ISSN: 2088-8694, DOI: 10.11591/ijpeds.v17.i4.pp2570-2580

An efficient and sustainable induction heating for lead melting: design, optimization, and application

Juthathip Haema[1], Rattanakorn Chantawarang[2]
[1]Department of Electrical Engineering Technology, College of Industrial Technology,
King Mongkut's University of Technology North Bangkok, Bangkok, Thailand
[2]Department of Electronics Engineering Technology, College of Industrial Technology,
King Mongkut's University of Technology North Bangkok, Bangkok, Thailand

Article Info

Article history:

Received Apr 25, 2026
Revised Aug 26, 2026
Accepted Sep 13, 2026

Keywords:

Half-bridge inverter
High frequency transformers
Induction heating
Pulse width modulation
Resonant inverter

ABSTRACT

This paper presents the design and development of a high-frequency half-bridge inverter for lead melting applications. The proposed system includes a step-down transformer, a full-bridge rectifier, a pulse-width modulation (PWM) control unit, a MOSFET-based half-bridge inverter, a high-frequency transformer, and an induction-heating load. We experimentally validated the system using 300-gram samples of lead-antimony alloy, lead-tin alloy, and recycled lead. All samples completely melted within 120 seconds. The lead–antimony alloy achieved the highest temperature of 240.6 °C, followed by lead tin alloy at 231.2 °C and recycled lead a 215.3 °C. The system delivered approximately 750 W output power with an efficiency of up to 98%. The results demonstrate that the proposed inverter provides stable operation and high efficiency, making it suitable for small- and medium-scale lead melting applications.

This is an open access article under the CC BY-SA license.

Corresponding Author:

Rattanakorn Chantawarang
Department of Electronics Engineering Technology, College of Industrial Technology
King Mongkut's University of Technology North Bangkok
Bangkok, Thailand
Email: rattanakorn.p@cit.kmutnb.ac.th

1. INTRODUCTION

The economy of Thailand has experienced steady growth, particularly in the agriculture, commerce, and industrial sectors. As previously mentioned, businesses can be classified into three categories: large enterprises, medium-sized enterprises, and small enterprises [1]. Among these, small and medium-sized enterprises (SMEs) play a crucial role in driving the national economy, especially in manufacturing and metal processing industries. This study focuses on SMEs, as they represent the primary users of induction heating technologies, particularly in small-scale metal processing applications such as lead melting for battery production and recycling processes [2]-[5]. Induction heating is widely applied in the thermal processing of tools and metal products, including melting, hardening, forging, and machining. In lead melting applications, a crucible typically made of graphite or graphite-based composites is used to contain the metal during the heating process. A time-varying magnetic field generated by an induction coil induces eddy currents within the crucible and/or the metal charge, producing heat through resistive losses. This mechanism enables efficient and controllable heating, which is essential for achieving consistent melting quality and minimizing material loss. High-frequency induction heating is increasingly adopted due to its superior efficiency and effectiveness. Compared with conventional fuel-based heating methods, such as gas or oil furnaces, induction heating offers significant advantages [6]. Heat can be applied precisely to a specific region or confined within the crucible without direct contact with the energy source, as it is generated internally within the material.

This results in faster heating rates, improved temperature control, and enhanced energy efficiency. In addition, the absence of combustion eliminates smoke, harmful emissions, and contamination, thereby improving workplace safety and environmental sustainability [7].

Although half-bridge inverter topologies have been widely studied, this work focuses on system-level optimization for induction heating in lead melting applications, particularly for small- to medium-scale industries. The main contributions of this study include: i) The design of a high-efficiency induction heating system operating at optimized frequency conditions; ii) Experimental validation using different lead materials; and iii) Analysis of thermal performance and energy efficiency. These contributions provide practical insights into the development of cost-effective and sustainable induction heating systems [8].

2. BASIC AND PROPOSED INDUCTION HEATING TOPOLOGY

Induction heating is a non-contact heating technique based on the principles of electromagnetism, in which heat is generated within a conductive material through electromagnetic induction. The fundamental mechanism is governed by Faraday's law of electromagnetic induction and Lenz's law, which describes the generation of an electromotive force (EMF) in response to a time-varying magnetic field [9]. When an alternating current flows through an induction coil, it produces a time-varying magnetic field surrounding the coil. When a conductive material, such as a metal workpiece or a graphite crucible, is placed within this magnetic field, an induced current known as an eddy current is generated within the material. These currents circulate within the material and generate heat due to electrical resistance, according to Joule's law. In addition to resistive (Joule) heating, magnetic materials may also experience hysteresis losses due to repeated magnetization and demagnetization cycles [10]. However, for non-ferromagnetic materials such as lead, the dominant heating mechanism is eddy current loss, as illustrated in Figure 1.

An induction heating system consists of key components: a high-frequency power supply, an induction coil, a workpiece or crucible, and a cooling system. The power supply converts electrical energy into high-frequency alternating current, which flows through the coil to generate a magnetic field. Heating efficiency depends on factors such as operating frequency, electrical resistivity, magnetic permeability, and the geometry of the coil and load. A key phenomenon is the skin effect, where induced current concentrates near the material surface. The penetration depth depends on material properties and frequency: higher frequencies produce shallow heating, while lower frequencies allow deeper heat distribution. In applications like lead melting, a graphite or composite crucible is used to contain the metal. The crucible can act as a susceptor, absorbing induced currents and transferring heat to the metal. This enables fast, efficient, and controllable heating, making induction heating suitable for industrial processes [11]-[15]. As frequency increases, skin depth decreases, confining heat to the surface. At lower frequencies, heat penetrates deeper. Therefore, selecting an appropriate frequency is essential for achieving the desired heating profile and efficiency [16]. A high-frequency half-bridge inverter is designed to control the operating frequency, ensuring efficient energy transfer and optimal thermal performance, as shown in Table 1.

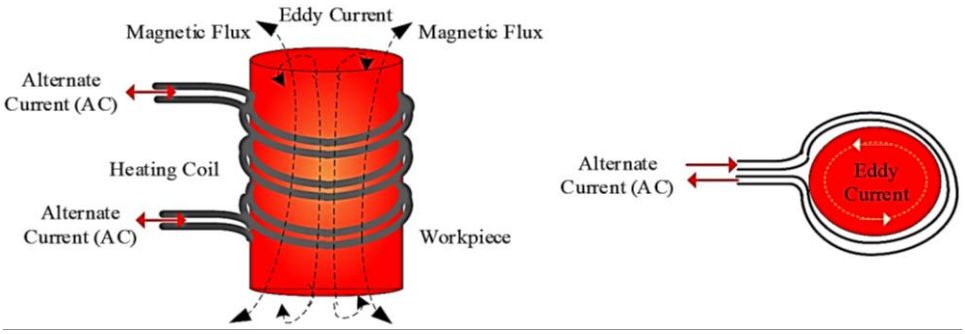

Figure 1. Basics of induction heating

Table 1. Comparison between low frequency and high frequency

Parameters	Low frequency	High frequency
Frequency range	~50 Hz to several kHz	~10 kHz to several hundred kHz
Skin depth	Deep	Shallow
Heat distribution	Heat spreads throughout the workpiece	Heat concentrated near the surface
Workpiece size	Large	Small
Typical applications	Metal melting, forging	Surface hardening, annealing, heating of small parts

2.1. Types of crucibles for lead melting in induction heating

In induction heating applications for lead melting, crucibles can be classified into several types based on their material composition and functional characteristics [17]. The selection of a suitable crucible is essential, as it directly affects heating efficiency, contamination, durability, and overall system performance. As displayed in Table 2. The main types of crucibles used in induction heating are as follows:

i) Graphite crucible

Graphite crucibles are widely used in induction heating applications due to their excellent thermal conductivity and high temperature resistance. They are capable of absorbing induced currents and acting as a susceptor, thereby efficiently transferring heat to the molten lead. These crucibles offer several advantages, including high thermal conductivity, good resistance to thermal shock, and suitability for induction heating processes. However, they also have certain limitations, such as susceptibility to oxidation at elevated temperatures and relatively higher cost compared to some ceramic materials.

ii) Clay-graphite crucible

Clay-graphite crucibles are composed of a mixture of graphite and refractory clay and are the most commonly used type in small- and medium-scale lead melting applications. They offer several advantages, including good resistance to thermal shock, lower cost compared to pure graphite crucibles, and adequate mechanical strength. However, they also present certain limitations, such as lower thermal conductivity and slightly lower purity compared to pure graphite materials.

iii) Silicon carbide–graphite crucible (SiC–graphite)

Graphite combined with silicon carbide, forming a composite material with enhanced mechanical strength and improved oxidation resistance. They offer several advantages, including high mechanical strength, excellent resistance to oxidation and corrosion, and a long service life. However, they also have certain limitations, such as higher cost and slightly lower thermal conductivity compared to pure graphite.

iv) Ceramic crucible

Ceramic crucibles, such as alumina or zirconia, are electrically insulating materials. In induction heating applications, they do not generate heat directly but rely on the heated metal or an external susceptor for heat transfer. They offer several advantages, including high chemical stability, high purity, and low contamination. However, they also present certain limitations, such as poor resistance to thermal shock and lower efficiency in induction heating systems.

Table 2. Summarizes the types of crucibles for lead melting

Type	Induction efficiency	Purity	Durability	Typical use
Graphite	High	High	High	Widely used
Clay-graphite	Medium–high	Medium	High	Most common
SiC–graphite	High	High	Very high	Industrial
Ceramic	Low	Very high	Medium	Laboratory

In this study, graphite crucibles were selected due to their ability to efficiently transfer heat to the molten lead. In addition, their high thermal conductivity and excellent resistance to rapid temperature changes make them particularly suitable for induction heating applications [18]. These characteristics promote efficient and relatively uniform heat distribution within the crucible, thereby facilitating the rapid melting of lead while reducing the likelihood of thermal stresses caused by abrupt temperature variations. Consequently, graphite crucibles provide a thermally stable environment that supports consistent heating conditions throughout the experimental process.

2.2. The circuit of a half-bridge inverter

This study aims to present an induction heating system for lead melting. The proposed system achieves efficient, controllable, and uniform heating performance and comprises six key components, each playing a critical role in the overall operation. First, a step-down transformer is employed to reduce the input voltage from 230 Vac to 110 Vac at 50 Hz. This reduction ensures compatibility with the subsequent power conversion stages and enhances system safety. Second, a full-bridge rectifier is used to convert the alternating current (AC) into direct current (DC), providing a stable DC supply for the inverter stage. Third, a pulse width modulation (PWM) control signal is generated to drive the switching devices. This control unit regulates the switching frequency and duty cycle, allowing precise control of the output power and enabling the system to operate near resonance for improved efficiency. The PWM signal is then fed into a gate-drive circuit, which ensures proper switching of the power semiconductor devices. Fourth, a half-bridge inverter employing power MOSFETs is utilized to convert the DC voltage into high-frequency alternating current. This high-frequency AC is essential for generating a time-varying magnetic field in the induction coil. The

use of MOSFETs enables high switching speed, reduced switching losses, and improved overall system efficiency. Fifth, a high-frequency transformer is incorporated to provide electrical isolation between the power source and the load, thereby enhancing safety. In addition, it helps balance the voltage supplied to the induction coil and can be used for impedance matching, which is important for maximizing power transfer efficiency [19]. Finally, the induction coil is employed as the heating element for the lead melting process, as illustrated in Figure 2.

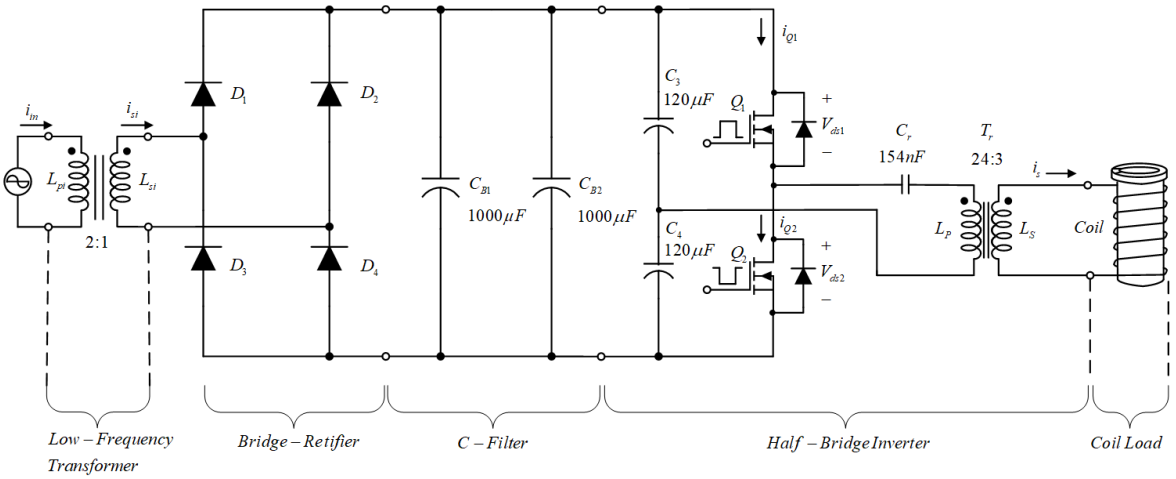

Figure 2. Circuit diagram for induction heating

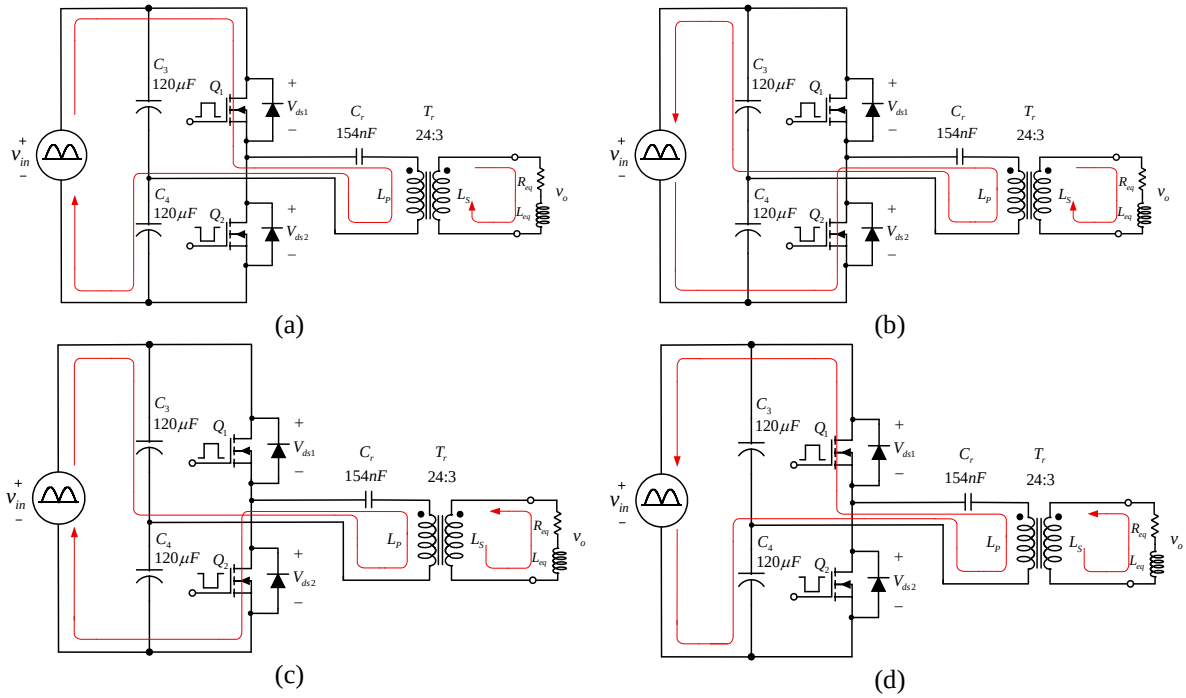

Figure 3. Operation mode of half-bridge inverter: (a) Mode 1, (b) Mode 2, (c) Mode 3, and (d) Mode 4

The operating modes of the half-bridge inverter circuit are shown in Figure 3.

– Mode 1: When switch Q_1 is turned on while Q_2 remains off, the current flows from the DC bus (Vbus) through the upper switch Q_1, then passes through the resonant capacitor (Cr) and the primary inductance (Lp). The current continues through the transformer primary, transferring energy to the secondary winding (Ls) and the load. During this interval, the resonant tank is actively excited, and energy is delivered to the output, as illustrated in Figure 3(a).

- Mode 2: When both Q_1 and Q_2 are turned off, the current in the resonant inductor cannot cease instantaneously. As a result, the stored energy in the magnetizing and resonant inductances forces the current to flow through the body diode of Q_2 (D_{Q2}). The primary current continues circulating through the resonant path, and energy is still transferred to the secondary side. This interval supports soft switching by allowing voltage transition across the switches, as presented in Figure 3(b).
- Mode 3: When switch Q_2 is turned on while Q_1 is off, the current flows from the DC bus through the lower switch Q_2, then through the resonant capacitor (Cr) and primary inductance (Lp), but in the opposite direction compared to mode 1. The transformer is excited in reverse polarity, and energy is again transferred to the secondary winding (Ls) and load, as demonstrated in Figure 3(c).
- Mode 4: When both switches are turned off again, the energy stored in the inductances sustains the current flow. The current now commutates through the body diode of Q_1 (D_{Q1}), completing the resonant cycle. The primary current continues to supply energy to the secondary side while gradually decaying, preparing the circuit to return to mode 1, as displayed in Figure 3(d).

2.3. Resonant tank analysis

The proposed half-bridge inverter operates based on a series resonant tank composed of the resonant capacitor (Cr) and the primary inductance (Lp). The purpose of the resonant tank is to shape the current waveform into a sinusoidal form, thereby reducing switching losses and improving overall system efficiency. The resonant frequency of the circuit is defined as (1):

$$f_r = \frac{1}{2\pi\sqrt{L_p C_r}} \tag{1}$$

where Lp represents the primary inductance, and Cr is the resonant capacitance. In this study, the system is designed to operate close to the resonant frequency to achieve maximum power transfer and efficient energy conversion. The impedance of the resonant tank can be expressed as (2):

$$Z = \sqrt{R^2 + \left(\omega L_p - \frac{1}{\omega C_r}\right)^2} \tag{2}$$

where R represents the equivalent load resistance reflected to the primary side, and $\omega = 2\pi f$is the angular frequency. At resonance ($\omega = \omega_r$), the inductive and capacitive reactance cancel each other, resulting in minimum impedance and maximum current flow through the circuit. Under this condition, the current flowing through the resonant tank becomes nearly sinusoidal, which is beneficial for reducing harmonic distortion and electromagnetic interference. Moreover, operating near resonance enables soft-switching conditions such as zero voltage switching (ZVS), where the MOSFETs are turned on at near-zero voltage, significantly reducing switching losses and improving efficiency. The resonant behavior also plays a critical role in controlling the power delivered to the load. By adjusting the switching frequency relative to the resonant frequency, the output power can be regulated without the need for additional control complexity. This makes the proposed system suitable for compact and energy-efficient induction heating applications [20]-[22].

3. RESULTS AND DISCUSSION

The block diagram of the proposed induction heating system for lead melting is illustrated in Figure 4. The system employs a half-bridge resonant inverter specifically designed for induction heating applications. The inverter operates based on high-frequency switching, generating an alternating current within the resonant tank circuit, which consists of a resonant capacitor and a high-frequency transformer [23], [24]. Table 3 summarizes the main electrical parameters and design specifications used in the proposed circuit.

The experiments used three types of lead: lead–antimony alloy, lead–tin alloy, and recycled lead:

i) The lead–antimony alloy is formed by adding antimony (Sb) to lead to improve hardness and mechanical strength. Compared to pure lead, it exhibits greater rigidity and enhanced wear resistance. This alloy is commonly used in battery grids, bullets, and cast components requiring high mechanical durability.
ii) The lead–tin alloy is produced by combining lead with tin (Sn), which improves fluidity and reduces the melting temperature. Consequently, it provides excellent casting performance and is widely applied in soldering and precision casting.
iii) Recycled lead is obtained from the reprocessing of scrap materials, such as used batteries. Although it is cost-effective, its composition may vary due to impurities. Therefore, proper refining and quality control are essential to ensure consistent material properties for industrial use.

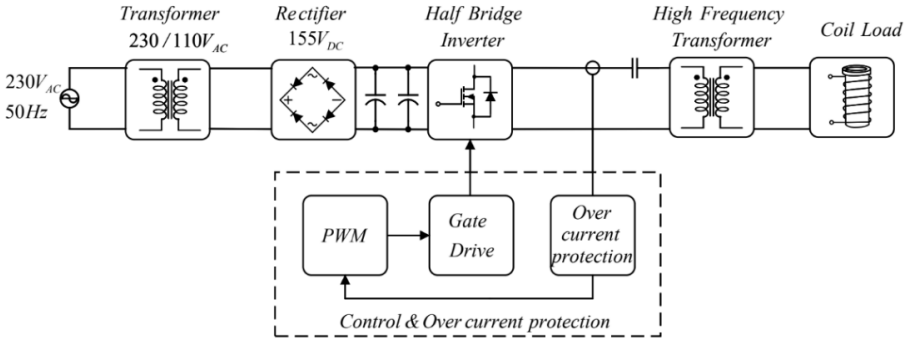

Figure 4. Block diagram for induction heating

Table 3. Summarizes the design parameters in the circuit

Parameters	Device number and value in the circuit
Vi_{rms}	230 V_{AC}/ 50 Hz
V_{bus}	155 V_{DC}
D_1, D_2, D_3, D_4	KBPC5010
M1, *M2*	IRFP460
High transformer	EE65/66/27
Capacitance resonant *Cr*	154 nF
Turn ratio	24 : 3
Workpiece	- lead antimony alloy - lead-tin alloy - recycled lead
Frequency	50 kHz

3.1. Measurement of the output circuit as a lead-antimony alloy load

The circuit of the half-bridge resonant inverter, along with its corresponding output voltage, output current, and temperature measurements, is presented in Figure 5. As shown in Figure 5(a), the measured output voltage is approximately 70 Vrms, with a corresponding current of 12.06 A. After 120 seconds of operation, the temperature of the lead inside the system reaches 240.6 °C as in Figure 5(b). The molten lead exhibited a slightly cloudy and shiny appearance as in Figure 5(c).

The results for the lead–antimony alloy indicate that the sample had an initial mass of 300 grams before melting, which slightly decreased to 298.2 grams after the melting process, as shown in Figure 5(d). This minor mass reduction may be attributed to material loss during heating, such as oxidation, evaporation, or fume generation at elevated temperatures.

3.2. Measurement of the output circuit as a lead-tin alloy load

The circuit of the half-bridge resonant inverter and its corresponding output voltage, current, and temperature measurement results are illustrated in Figure 6. As shown in Figure 6(a), the output voltage is approximately 75 Vrms, with a corresponding current of 12.02 A. After 120 seconds of operation, the temperature of the lead within the system increases to 231.2 °C as in Figure 6(b). The appearance of the lead is clear and shiny, as in Figure 6(c).

Lead-tin alloy results indicate that the lead sample had an initial mass of 300 grams prior to melting, which slightly decreased to 299.2 grams after the melting process, as displayed in Figure 6(d). This minor reduction in mass may be attributed to material loss during heating, such as oxidation, evaporation, or the formation of fumes at elevated temperatures.

3.3. Measurement of the output circuit using recycled lead load

The circuit of the half-bridge resonant inverter and its corresponding output voltage, current, and temperature measurement results are illustrated in Figure 7. As shown in Figure 7(a), the output voltage is approximately 74.7 Vrms, with a corresponding current of 11.79 A. After 120 seconds of operation, the temperature of the lead within the system increases to 215.3 °C as in Figure 7(b). The appearance of the lead is clear and shiny, as in Figure 7(c). Lead-tin alloy results indicate that the lead sample had an initial mass of 300 grams prior to melting, which slightly decreased to 299.2 grams after the melting process, as displayed in Figure 7(d). This minor reduction in mass may be attributed to material loss during heating, such as oxidation, evaporation, or the formation of fumes at elevated temperatures.

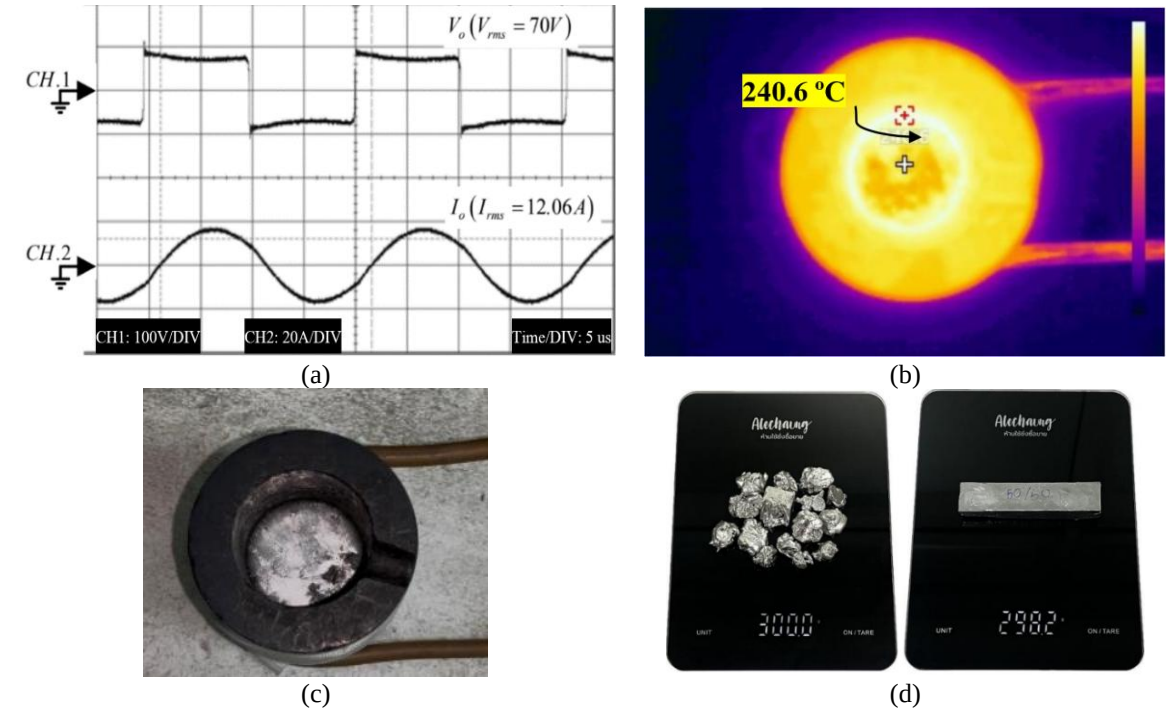

Figure 5. Measurement for induction heating using a lead-antimony alloy load: (a) measured output voltage and current waveforms, (b) thermal image from the thermal camera, (c) thermal image of the experiment, and (d) lead before and after the experiment

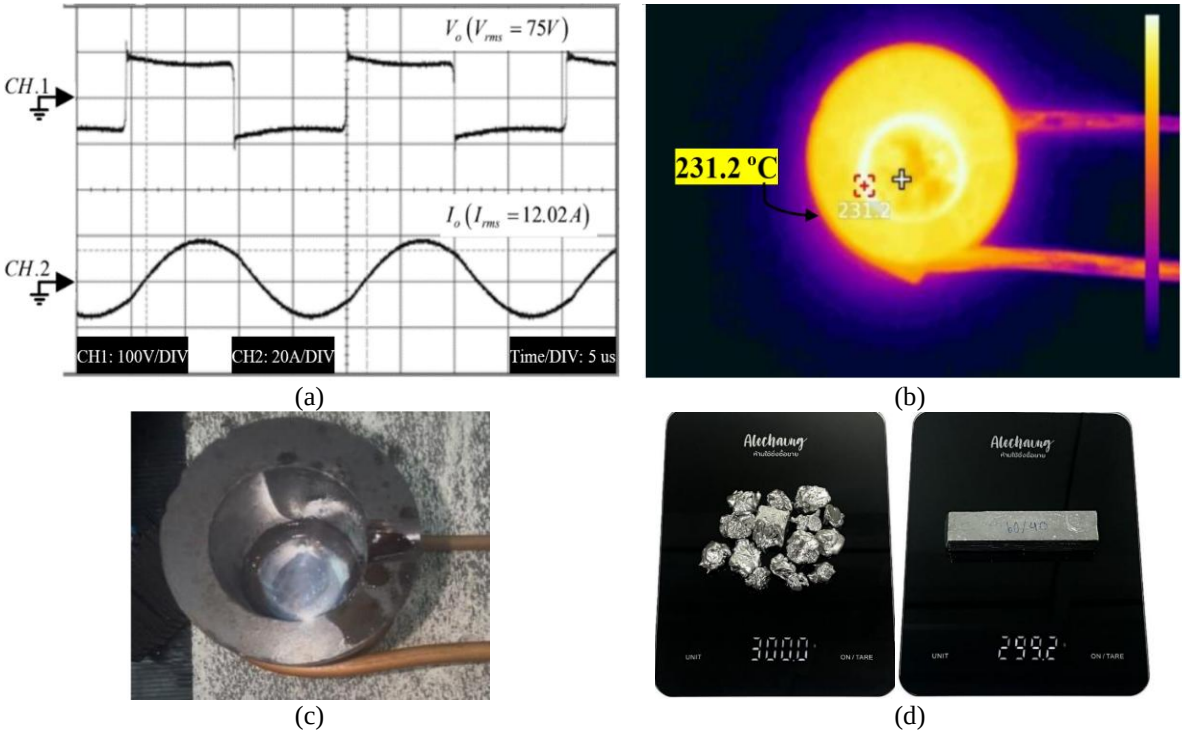

Figure 6. Measurement for induction heating using a lead-tin alloy load: (a) measured output voltage and current waveforms, (b) thermal image from the thermal camera, (c) thermal image of the experiment, and (d) lead before and after the experiment

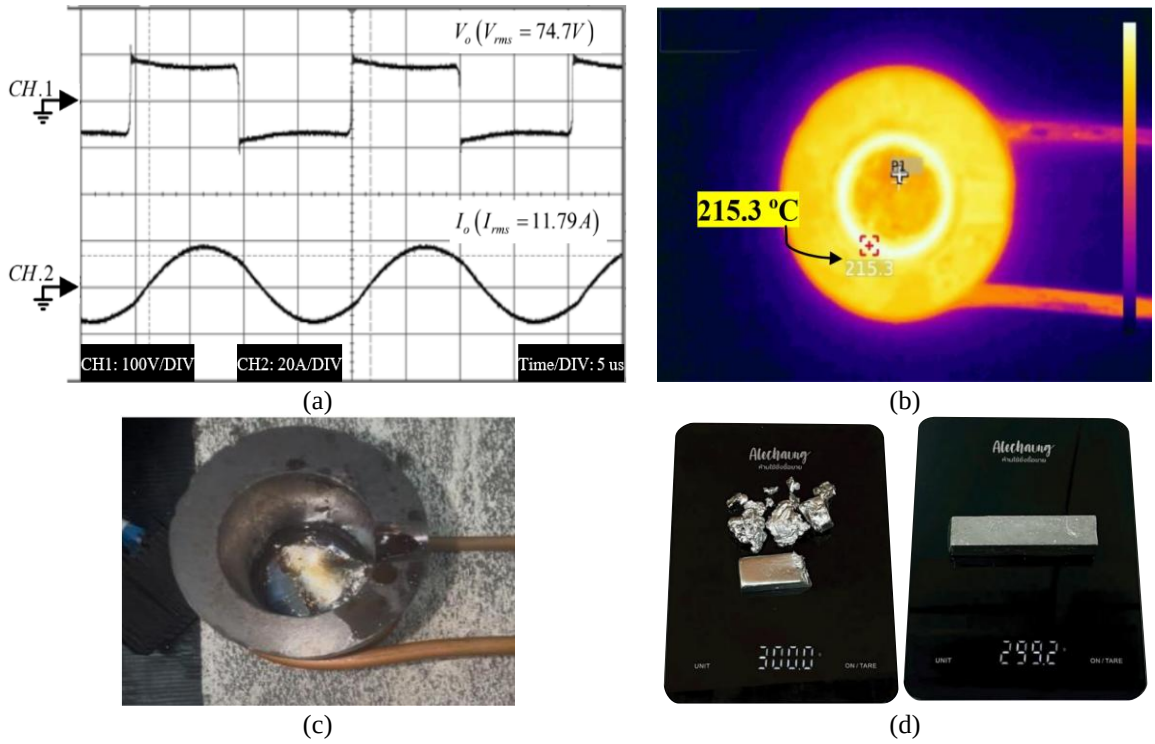

Figure 7. Measurement for induction heating as use recycled lead load: (a) measured output voltage and current waveforms, (b) thermal image of the thermal camera, (c) thermal image of the experimental, and (d) lead before and after the experiment

3.4. Compare types of lead in the circuit and temperature of workpiece

Table 4 summarizes the output voltage, output current, temperature, and efficiency of the induction heating system for different types of lead materials over time (10, 60, and 120 seconds). Overall, the results show that temperature increases significantly with heating time for all lead types, while the output voltage and current remain relatively stable with only minor fluctuations. Among the materials, the lead–tin alloy exhibits the highest efficiency at 98.4%, followed by recycled lead at 98.2% and lead–antimony alloy at 97.5%.

In terms of thermal performance, the lead–antimony alloy reaches the highest temperature at 120 seconds at 240.6 °C, indicating better heat absorption or retention compared to the other materials. The lead–tin alloy shows slightly lower final temperatures at 231.2 °C, while recycled lead has the lowest temperature at 215.3 °C at the same time interval. These results suggest that although all materials demonstrate stable electrical behavior, their thermal responses and efficiencies differ, with lead–tin alloy offering the best efficiency and lead–antimony alloy providing the highest heating performance.

Based on the experimental results, the system is capable of melting 300 grams of lead within 120 seconds while maintaining a high efficiency of approximately 98% and stable output power around 750 W. These characteristics indicate that the system can significantly reduce processing time and energy consumption compared to conventional fuel-based furnaces commonly used in SMEs. Furthermore, the compact design and high-frequency operation enable localized heating, which minimizes heat loss and improves overall thermal efficiency. This makes the proposed system highly suitable for small-scale metal processing applications such as battery recycling and casting processes, where precise temperature control and energy savings are essential.

Crucible temperature measurements revealed clear differences in the thermal behavior of the tested lead materials during melting. The temperature rise (ΔT) reflects the amount of heat absorbed and retained by the crucible. The lead–antimony alloy shows the highest ΔT (80.6 °C), indicating that more thermal energy is required to reach and maintain the molten state. This is likely due to antimony increasing hardness and thermal stability, which broadens the melting range. The lead–tin alloy exhibits a moderate ΔT (68.2 °C), suggesting better melting efficiency. This aligns with the role of tin in improving fluidity and lowering the melting temperature. In contrast, recycled lead has the lowest ΔT (45.3 °C), indicating lower energy demand or faster heat transfer. This may result from compositional variations, impurities or the presence of low-melting-point

elements. Overall, material composition strongly affects heat absorption, melting behavior, and thermal efficiency during smelting.

To further evaluate the performance of the proposed system, a comparison with other inverter topologies reported in the literature is presented in Table 5, such as full-bridge and resonant converters, is considered. Previous studies have reported efficiencies in the range of 90–95%, whereas the proposed system achieves up to 98% efficiency under similar operating conditions [25]-[27]. This indicates that the proposed design provides improved energy utilization and reduced losses. In addition, practical considerations such as scalability and cost-effectiveness are important for real-world applications. The proposed system is suitable for SMEs due to its relatively simple topology, low component count, and high efficiency. Compared to conventional fuel-based furnaces, the system offers reduced energy consumption and lower environmental impact.

Table 4. Summarizes the output voltage, output current, temperature, and efficiency in the circuit

Type of lead	Time (s)	Output voltage (V)	Output current (A)	Temperature inside (℃)	Temperature outside (℃)	Efficiency (%)
Lead-antimony alloy	10	73.0	11.91	68.30	43.0	97.5
	60	71.7	11.84	193.7	130	
	120	70.0	12.06	240.6	160	
Lead-tin alloy	10	70.4	11.98	61.00	43.0	98.4
	60	71.2	11.82	183.4	135	
	120	75.0	12.02	231.2	163	
Recycled lead	10	72.1	11.91	61.90	43.0	98.2
	60	71.4	11.80	181.9	132	
	120	74.7	11.79	215.3	170	

Table 5. Summarizes the comparison of different inverter topologies

Topology	Power (W)	Efficiency (%)
Full-bridge inverter	500-1000	90-95
LLC resonant inverter	500-1200	92-96
Proposed half-bridge inverter	750	98

4. CONCLUSION

The high-frequency half-bridge inverter developed for lead smelting applications consists of six key components: a step-down transformer, a full-wave bridge rectifier, a PWM signal generator for control, a half-bridge inverter employing power MOSFETs, a high-frequency transformer, and the workpiece (heating load). The proposed system operates at high frequency to enhance energy transfer efficiency and enable rapid localized heating. In the experimental study, 300 grams samples of three different types of lead materials-lead-antimony alloy, lead-tin alloy, and recycled lead were investigated. The results show that all samples completely melted within 120 seconds of operation. The lead–antimony alloy reached the highest temperature of 240.6 °C, followed by the lead–tin alloy at 231.2 °C, and recycled lead at 215.3 °C, indicating variations in thermal response due to differences in material composition and properties. Furthermore, the developed high-frequency half-bridge inverter demonstrated stable and reliable performance throughout the experiments. The system consistently delivered an output power in the range of approximately 750 W under full-load conditions, with an overall energy efficiency of around 98%. This high efficiency highlights the effectiveness of the proposed system in minimizing energy losses while maintaining strong heating capability, making it suitable for small to medium-scale lead smelting applications.

FUNDING INFORMATION

The authors gratefully acknowledge students at PElectronicsX Lab and the College of Industrial Technology, King Mongkut's University of Technology North Bangkok, for supporting this work.

AUTHOR CONTRIBUTIONS STATEMENT

This journal uses the Contributor Roles Taxonomy (CRediT) to recognize individual author contributions, reduce authorship disputes, and facilitate collaboration.

Name of Author	C	M	So	Va	Fo	I	R	D	O	E	Vi	Su	P	Fu
Juthathip Haema	✓	✓		✓	✓	✓	✓	✓	✓	✓	✓	✓	✓	
Rattanakorn Chantawarang	✓	✓		✓	✓	✓	✓	✓		✓	✓	✓		

C : **C**onceptualization
M : **M**ethodology
So : **So**ftware
Va : **Va**lidation
Fo : **Fo**rmal analysis
I : **I**nvestigation
R : **R**esources
D : **D**ata Curation
O : Writing - **O**riginal Draft
E : Writing - Review & **E**diting
Vi : **Vi**sualization
Su : **Su**pervision
P : **P**roject administration
Fu : **Fu**nding acquisition

CONFLICT OF INTEREST STATEMENT

Authors state no conflict of interest.

DATA AVAILABILITY

The authors confirm that the data supporting the findings of this study are available within the article.

REFERENCES

[1] V. Rudnev, D. Loveless, and R. L. Cook, *Handbook of induction heating, second edition*. Boca Raton, FL: CRC Press, 2017, doi: 10.1201/9781315117485.

[2] E. Rapoport and Y. Pleshivtseva, *Optimal control of static induction heating processes*. Boca Raton, FL: CRC Press, 2020, doi: 10.1201/9781420019490-8.

[3] J. Haema and R. Phadungthin, "High frequency induction heating via split helical coil using full bridge inverter," in *PEET 2025 - Proceedings of 2025 International Conference on Power Engineering and Electrical Technology*, 2025, doi: 10.1109/PEET65412.2025.11341373.

[4] A. Pascual, J. Acero, C. Carretero, S. Llorente, and J. M. Burdio, "Electromagnetic modeling and analysis of multimaterial cookware for domestic induction heating," *IEEE Access*, vol. 11, pp. 79275–79284, 2023, doi: 10.1109/ACCESS.2023.3298571.

[5] A. Rattanaudompisut and P. Charoenwiangnuea, "Experimental study on induction heating generation for plastic deformation," *Materials Today: Proceedings*, 2023, doi: 10.1016/j.matpr.2023.09.022.

[6] B. Saha and R. Y. Kim, "High power density series resonant inverter using an auxiliary switched capacitor cell for induction heating applications," *IEEE Transactions on Power Electronics*, vol. 29, no. 4, pp. 1909–1918, 2014, doi: 10.1109/TPEL.2013.2265984.

[7] H. Sarnago, O. Lucia, A. Mediano, and J. M. Burdio, "Efficient and cost-effective ZCS direct AC-AC resonant converter for induction heating," *IEEE Transactions on Industrial Electronics*, vol. 61, no. 5, pp. 2546–2555, 2014, doi: 10.1109/TIE.2013.2262752.

[8] U. T. Shami and T. A. Shami, "An adaptive load-matching method for the induction heating coil with DC power supply," *International Journal of Circuit Theory and Applications*, vol. 52, no. 10, pp. 5025–5041, 2024, doi: 10.1002/cta.4005.

[9] X. Chen, J. Wang, B. Ma, Z. Duan, and H. Wang, "Research status and applications of dual-frequency induction heating power supply," *Electronics (Switzerland)*, vol. 13, no. 24, 2024, doi: 10.3390/electronics13244913.

[10] P. K. Sadhu, P. Pal, N. Pal, and S. Sanyal, "Selection of power semiconductor switches in M.H.B.R.I. fitted induction heater for less harmonic injection in power line," *International Journal of Power Electronics and Drive Systems*, vol. 6, no. 1, pp. 121–128, 2015, doi: 10.11591/ijpeds.v6.i1.pp121-128.

[11] E. J. Dede *et al.*, "Soft switching series resonant converter for induction heating applications," in *Proceedings of the International Conference on Power Electronics and Drive Systems*, 1995, pp. 689–693, doi: 10.1109/peds.1995.404986.

[12] H. Sarnago, O. Lucia, and J. M. Burdio, "A versatile resonant tank identification methodology for induction heating systems," *IEEE Transactions on Power Electronics*, vol. 33, no. 3, pp. 1897–1901, Mar. 2018, doi: 10.1109/TPEL.2017.2740998.

[13] H. Sarnago, Ó. Lucía, and J. M. Burdío, "A comparative evaluation of sic power devices for high-performance domestic induction heating," *IEEE Transactions on Industrial Electronics*, vol. 62, no. 8, pp. 4795–4804, 2015, doi: 10.1109/TIE.2015.2405057.

[14] J. Acero, R. Alonso, L. A. Barragán, and J. M. Burdío, "Modeling of planar spiral inductors between two multilayer media for induction heating applications," *IEEE Transactions on Magnetics*, vol. 42, no. 11, pp. 3719–3729, 2006, doi: 10.1109/TMAG.2006.882308.

[15] O. Lucia, P. Maussion, E. J. Dede, and J. M. Burdio, "Induction heating technology and its applications: past developments, current technology, and future challenges," *IEEE Transactions on Industrial Electronics*, vol. 61, no. 5, pp. 2509–2520, 2014, doi: 10.1109/TIE.2013.2281162.

[16] B. W. Williams, *Power electronics devices drivers and applications*, New York: Mac Millan, 1992.

[17] S. Chudjuarjeen, A. Sangswang, and C. Koompai, "An improved LLC resonant inverter for induction heating with asymmetrical control," *IEEE International Symposium on Industrial Electronics*, vol. 58, no. 7, pp. 1612–1617, 2009, doi: 10.1109/ISIE.2009.5222544.

[18] H. N. Pham, H. Fujita, K. Ozaki, and N. Uchida, "Dynamic analysis and control for resonant currents in a zone-control induction heating system," *IEEE Transactions on Power Electronics*, vol. 28, no. 3, pp. 1297–1307, 2013, doi: 10.1109/TPEL.2012.2210286.

[19] N.-J. Park, D.-Y. Lee, and D.-S. Hyun, "A power-control scheme with constant switching frequency in class-d inverter for induction-heating jar application," *IEEE Transactions on Industrial Electronics*, vol. 54, no. 3, pp. 1252–1260, Jun. 2007, doi: 10.1109/TIE.2007.892741.

[20] C. H. Chang, E. C. Chang, C. A. Cheng, H. L. Cheng, and S. C. Lin, "Small signal modeling of LLC resonant converters based on extended describing function," in *Proceedings - 2012 International Symposium on Computer, Consumer and Control, IS3C 2012*, 2012, pp. 365–368, doi: 10.1109/IS3C.2012.99.
[21] C. Buccella, C. Cecati, H. Latafat, P. Pepe, and K. Razi, "Linearization of LLC resonant converter model based on extended describing function concept," in *2013 IEEE International Workshop on Inteligent Energy Systems (IWIES)*, IEEE, Nov. 2013, pp. 131–136, doi: 10.1109/IWIES.2013.6698574.
[22] H. Fujita, N. Uchida, and K. Ozaki, "A new zone-control induction heating system using multiple inverter units applicable under mutual magnetic coupling conditions," *IEEE Transactions on Power Electronics*, vol. 26, no. 7, pp. 2009–2017, Jul. 2011, doi: 10.1109/TPEL.2010.2101084.
[23] R. L. Steigerwald, "A comparison of half-bridge resonant converter topologies," *IEEE Transactions on Power Electronics*, vol. 3, no. 2, pp. 174–182, Apr. 1988, doi: 10.1109/63.4347.
[24] O. Lucía, J. M. Burdío, I. Millán, J. Acero, and L. A. Barragán, "Efficiency-oriented design of ZVS half-bridge series resonant inverter with variable frequency duty cycle control," *IEEE Transactions on Power Electronics*, vol. 25, no. 7, pp. 1671–1674, Jul. 2010, doi: 10.1109/TPEL.2010.2042461.
[25] [1] H. W. Koertzen, J. D. van Wyk, and J. A. Ferreira, "Design of the half-bridge, series resonant converter for induction cooking," in *Proceedings of PESC '95 - Power Electronics Specialist Conference*, IEEE, pp. 729–735, doi: 10.1109/PESC.1995.474899.
[26] S. Tian, F. C. Lee, and Q. Li, "Equivalent circuit modeling of LLC resonant converter," in *2016 IEEE Applied Power Electronics Conference and Exposition (APEC)*, IEEE, Mar. 2016, pp. 1608–1615, doi: 10.1109/APEC.2016.7468082.
[27] M. Rajaram. and N. Booma, "Resonant inverter for induction heating," in *2012 International Conference on Computing, Electronics and Electrical Technologies (ICCEET)*, IEEE, Mar. 2012, pp. 358–366, doi: 10.1109/ICCEET.2012.6203832.

BIOGRAPHIES OF AUTHORS



Juthathip Haema received her Bachelor of Engineering degree from the College of Industrial Technology, King Mongkut's University of Technology North Bangkok, Thailand, in 2005, and her Master of Science degree from the Sirindhorn International Thai-German Graduate School of Engineering at the same university in 2009. She is a lecturer at the College of Industrial Technology, King Mongkut's University of Technology North Bangkok, Thailand. Her research interests include power converter topologies, power electronics applications, power system analysis, and asset management. She can be contacted at email: juthathip.h@cit.kmutnb.ac.th.



Rattanakorn Chantawarang received her Bachelor of Engineering degree from Chiang Mai University, Thailand, in 1993; her Master of Business degree from the University of Technology Sydney, Australia, in 1997; and her Master of Science and Doctor of Philosophy degrees from the Sirindhorn International Thai-German Graduate School of Engineering, King Mongkut's University of Technology North Bangkok, Thailand, in 2005 and 2013, respectively. She is a lecturer at the College of Industrial Technology, King Mongkut's University of Technology North Bangkok, Thailand. Her research interests include power system analysis, asset management, maintenance models, and power electronics. She can be contacted at email: rattanakorn.p@cit.kmutnb.ac.th.